Model Predictive Degree of Automation Regulation for Mobile Robots Using Robot Vitals and Robot Health

Braun, Christian Alexander; Ramesh, Aniketh; Rothfuss, Simon; Chiou, Manolis; Stolkin, Rustam; Hohmann, Soren

DOI:
10.1016/j.ifacol.2023.10.1025

Available online at www.sciencedirect.com

ScienceDirect

IFAC PapersOnLine 56-2 (2023) 8345–8350

Model Predictive Degree of Automation Regulation for Mobile Robots Using Robot Vitals and Robot Health

Christian Alexander Braun *,1 Aniketh Ramesh **,1
Simon Rothfuß * Manolis Chiou ** Rustam Stolkin **
Sören Hohmann *

* *Institute of Control Systems, Karlsruhe Institute of Technology, 76131 Karlsruhe, Germany (e-mail: christian.braun@kit.edu).*
** *Extreme Robotics Lab, School of Metallurgy and Materials Elm Rd, Birmingham B15 2SE (e-mail: axr1050@student.bham.ac.uk).*

Abstract: Environmental adversities can severely impact the performance of human-robot teams, potentially even leading to task failure. If the operator and the robot automation are not equally affected, adjusting the degree of automation to shift control authority between them is a means of maintaining the performance of the human-robot team. The robot vitals and robot health framework is a recent approach to quantifying runtime performance degradation in robots. This framework can serve as a methodological foundation for the adjustment of the degree of automation based on the human-robot system's state. In this paper, we contribute two model predictive adaptive automation systems that can adjust either the level or the degree of automation of a robot. These systems optimize robot health to ensure optimal performance of the human-robot team when exposed to adversities. Feasibility studies in simulation showcase the ability of our systems to manage the level and degree of automation, thus allowing for an optimal task execution by the human-robot team.

Keywords: Adaptive automation, Shared control, Cooperation, Degree of automation, Levels of autonomy, Levels of automation, Mixed initiative control.

1. INTRODUCTION

Robots are becoming increasingly capable of carrying out a wide variety of tasks autonomously. Remaining limitations in their autonomous capabilities, runtime performance degradation and other problematic situations during task execution can be addressed through remote human operator (i.e., tele-operator) assistance. Particularly during navigation tasks in extreme environments, a tele-operator can switch a Fully Autonomous (FA) robot to Manual Control (MC) to assist it with task execution. If the tele-operator is occupied elsewhere, or assistance is no longer required, the robot can be switched back to FA. Assisting robots by changing the extent of control an operator has over their actions, is called Level of Autonomy (LOA) Switching (Sheridan and Verplank (1978)). When describing such systems in existing literature, the words Autonomy and Automation are used interchangeably in this paper.

Shared control or input blending (Abbink et al. (2018)) can also be used to enable operator assistance for robots. In shared control, the robot's behaviour is determined by a ratio of control inputs from the tele-operator and the robot's onboard intelligence. For example, an operator can give the robot a general heading direction, and the robot's autonomy can ensure obstacles are avoided during navigation (Pappas et al. (2020)). Similarly, in mobile manipulation tasks, shared control can help mimic an operators actions while avoiding collisions and singularity positions (Rakita et al. (2019)).

LOA switching is employed if a robot occasionally requires assistance when they encounter problematic situations (Beer et al. (2014)). When continuous operator assistance or guidance is required for task execution, shared control is preferable (Udupa et al. (2021)). Combining both these control paradigms would yield a robust system that can find applications in a wider variety of tasks. In such a system, the ratio of control inputs (say α) could be varied based on the state of the human-robot system. If $\alpha = 0$, the robot would operate in MC. Increasing the value of α would allow different levels of shared control and $\alpha = 1$ would result in a FA robot. The ability to vary the extent of operator control over a robot's actions across the entire continuum between MC and FA is referred to as Degree of Autonomy (DOA) regulation (Wei et al. (1998)). Regulating a robot's LOA or DOA online during its runtime is cognitively demanding for a tele-operator (Delmerico et al. (2019)). Hence, a module to automatically regulate a robot's LOA or DOA during task execution would be useful.

In our paper, we contribute designs for modules that can assist a human operator with LOA or DOA regulation. Using the Robot Vitals and Robot Health framework

* This work was supported by the UKRI-EPSRC grant EP/R02572X/1 (UK National Centre for Nuclear Robotics).
[1] Christian Braun and Aniketh Ramesh are co-first authors.

10.1016/j.ifacol.2023.10.1025

(Ramesh et al. (2022)) for quantifying runtime performance degradation, we derive a model-predictive adaptive automation system that can automatically regulate a robot's autonomy to mitigate the effect of problematic situations during task execution. Finally, we present results from preliminary feasibility studies on this system.

2. LITERATURE REVIEW

Human-robot teams where the extent of operator engagement with the robot can be varied during runtime are called variable autonomy systems (Chiou et al. (2016)). Such systems are also known as adaptive autonomy (Cabrall et al. (2018)) or adjustable autonomy (Mostafa et al. (2019)) systems. Shared control (Musić and Hirche (2017)), Mixed Initiative (MI) Level of Autonomy switching (Chiou et al. (2021a); Jiang and Arkin (2015); Rothfuss et al. (2022)) and policy switching (Rigter et al. (2020)) are some implementations of variable autonomy systems. When applied to mobile robot navigation tasks, variable autonomy systems have demonstrated the potential to reduce total obstacle collisions (Pappas et al. (2020)) and cognitive workload (Chiou et al. (2021a)), improve task performance (Ruff et al. (2018)) and ease of use (Cabrall et al. (2018)). Evidence also suggests that variable autonomy systems can improve operator safety (Cabrall et al. (2018)), trust and transparency (Chiou et al. (2021b)).

Discretising the continuum between MC and FA into multiple LOAs can result in the loss of crucial information (Miller (2018)). Shared control can avoid this problem, by allowing autonomy regulation within a window of feasible options (referred to as ζ by Braun et al. (2019)). ζ can be chosen to prevent collisions during remote robot navigation (Pappas et al. (2020)), ensure safety and comfort while navigating unstructured environments (Udupa et al. (2021)), and even task specific motion assistance (Gao et al. (2014)). In our study we propose autonomy regulation systems for mobile robots LOAs or DOAs.

Regulation modules to adjust a robots DOA can be rule-based Chiou et al. (2021a), analytical (Braun et al. (2019)) or even machine learning based (Doroodgar et al. (2014)). Machine learning models require high fidelity simulations and large data sets to train. While rule-based models are relatively easier to design and deploy, such models are limited by the scope of rules generated. Therefore in our paper, we derive and contribute model predictive architectures for DOA and LOA regulation. Our model estimates the state of the robot, the environment and control inputs provided by the operator, and chooses the optimal DOA for the robot.

Automatically regulating autonomy has received some attention in the existing literature. A robot's LOA can be adjusted to maintain operator trust (Nikolaidis et al. (2017)), to tailor to operator expertise (Milliken and Hollinger (2017)), detect operator intention (Petousakis et al. (2020)) or context of operation (Gao et al. (2014)) and mitigate the effect of communication delays etc (Pappas et al. (2020)) etc. The literature suggests little agreement on the state estimation parameters or metrics used for assessing the right LOA, as these are highly contingent upon the application domain. Several studies have used metrics or formal methods to detect performance degradation in a human-robot system (Valero-Gomez et al. (2011); Zieba et al. (2011); Xiao et al. (2020)). However, these do not explicitly provide a single robot metric that can indicate the total performance degradation a robot is facing. In Ramesh et al. (2022), a set of metrics indicative of runtime performance degradation called 'robot vitals' are used to calculate the 'robot health' for mobile robots. The authors then demonstrate that robot health is a scalar estimate of the performance degradation a robot faces during runtime. Due to the robustness and scalability of this approach, we use it in our study.

3. PROBLEM STATEMENT

Fig. 1 illustrates the structure of the human-robot system considered in this work. Both the operator and the robot's controller provide their respective control inputs to the robot based on their observations of the system states. The 'Arbitration' module merges these control inputs and applies them to the robot. The ratio α of the control inputs is determined by the 'LOA / DOA Regulation' module based on robot health (Ramesh et al. (2022)).

The total probability of suffering of a robot P_{suf} can be calculated during runtime given the vitals v_i. The probability of suffering can then be used to compute the robot health. The LOA and DOA regulation modules use this information to adjust the value of α during runtime. Hence, we design the LOA and DOA regulation systems by optimising robot health $H : \mathbb{R}^{N_\text{v}} \to \mathbb{R}_{<0}$. This is accomplished by adjusting $\boldsymbol{\alpha}$ so that the N_v resultant robot vitals v_i compute to a higher value of robot health:

$$\boldsymbol{\alpha}^* = \underset{\boldsymbol{\alpha}}{\operatorname{argmax}}\ H\left(P_{\text{suf}}\left(v_1\left(\boldsymbol{x}\left(\boldsymbol{\alpha}\right), \boldsymbol{\alpha}\right), \dots\right)\right) \tag{1}$$

Please note that throughout this work time-dependencies of all variables are omitted for better readability. As this study is the first step towards DOA regulation using robot health, (1) is treated as a parameter optimisation problem instead of an optimal control problem.

Following Broggi et al. (2015), we model the considered robot with the following unicycle dynamics:

$$\dot{\boldsymbol{x}} = \begin{pmatrix} \dot{x} \\ \dot{y} \\ \dot{\theta} \end{pmatrix} = \begin{pmatrix} \cos(\theta) & 0 \\ \sin(\theta) & 0 \\ 0 & 1 \end{pmatrix} \boldsymbol{u} \tag{2}$$

Here, $\boldsymbol{x}$ denotes the robot's states with x and y representing its position in the two-dimensional coordinate frame and θ denoting its heading. The robot can be controlled via the inputs $\boldsymbol{u} = (\beta, \omega)^\top$ where β is the robot's velocity in the direction of the heading and ω is its angular velocity.

In this work, LOA and DOA regulation are studied on the action level of human-robot interaction. However, the principles developed in this work can be applied to other use cases, too. To implement different DOAs, we use linear policy blending $\boldsymbol{\Gamma} : \mathbb{R}^2 \times \mathbb{R}^2 \times [0,1]^2 \to \mathbb{R}^2$ to arbitrate the human input $\boldsymbol{u}_\text{H}$ and machine input $\boldsymbol{u}_\text{A}$ (Dragan and S.Srinivasa (2013)):

$$\boldsymbol{u} = \boldsymbol{\Gamma}\left(\boldsymbol{u}_\text{A}, \boldsymbol{u}_\text{H}, \boldsymbol{\alpha}\right) \tag{3}$$

$$\boldsymbol{\Gamma}_\text{pb}\left(\boldsymbol{u}_\text{A}, \boldsymbol{u}_\text{H}, \boldsymbol{\alpha}\right) = \begin{pmatrix} \alpha_1 u_{\text{A},1} + (1-\alpha_1)\, u_{\text{H},1} \\ \alpha_2 u_{\text{A},2} + (1-\alpha_2)\, u_{\text{H},2} \end{pmatrix} \tag{4}$$

Here, individual DOAs α_1 and α_2 are considered for the two dimensions of the input allowing for control authority

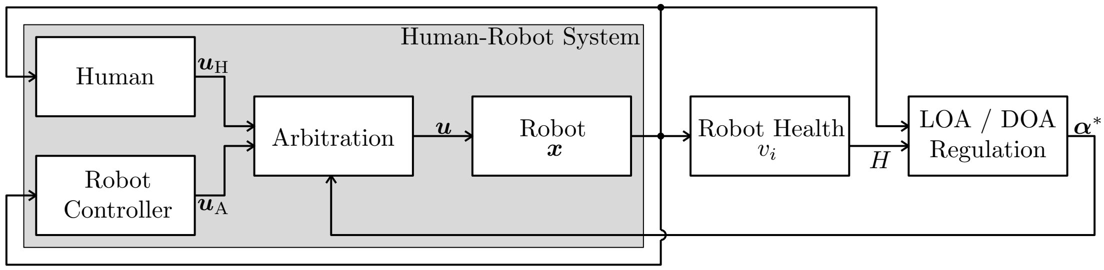

Fig. 1. Structure of the considered adaptive automation system.

shifts ranging from MC ($\alpha_i = 0$), over to shared control ($\alpha_i \in (0, 1)$) to a FA robot operation ($\alpha_i = 1$) in each of the two dimensions. LOAs with N_L levels can be implemented by setting $\boldsymbol{\alpha}$ to a certain value from a countable set $\Lambda = \{\boldsymbol{\alpha}_1, \ldots, \boldsymbol{\alpha}_{N_\mathrm{L}}\}$. This allows for the definition of the two problems considered in this work:

Problem 1. Adaptive Automation for LOA. Design a LOA regulation module optimizing (1) s.t. (2), (4) and models of $\boldsymbol{u}_\mathrm{H}(\boldsymbol{x})$ and $\boldsymbol{u}_\mathrm{A}(\boldsymbol{x})$ considering $\boldsymbol{\alpha} \in \Lambda$.

Problem 2. Adaptive Automation for DOA. Design a DOA regulation module optimizing (1) s.t. (2), (4) and models of $\boldsymbol{u}_\mathrm{H}(\boldsymbol{x})$ and $\boldsymbol{u}_\mathrm{A}(\boldsymbol{x})$ considering $\boldsymbol{\alpha} \in [0, 1]^2$.

4. MODEL PREDICTIVE ADAPTIVE AUTOMATION

The LOA and DOA regulation modules presented in this paper operate in a model predictive fashion. This is done to accommodate for robot health evaluating time spans (Ramesh et al. (2022)), and to utilize the model knowledge about the human-robot system contained in Problems 1 and 2. Both regulation modules predict the evolution robot health over a time horizon of length T_p to compute $\boldsymbol{\alpha}^*$. The optimal $\boldsymbol{\alpha}^*$ is then used for $T_s < T_p$.

4.1 LOA Model Predictive Adaptive Automation

Since the set Λ is countable, Problem 1 reduces to calculating robot health (H_i) N_L times for all $\boldsymbol{\alpha}_i \in \Lambda$ and then comparing the resulting H_i. The $\boldsymbol{\alpha}_i$ leading to the highest H_i is subsequently applied to the human-robot system. Fig. 2 shows the structure of the resulting Model Predictive Adaptive Automation for the LOA case (LOA-MPAA). Omitting potential model errors (i.e. assuming perfect models), this system is guaranteed to find the globally optimal solution. As the simulations of each of the human-robot system models are independent of each other, they can easily be executed in parallel. In practice, N_L is usually limited to less than ten levels (Vagia et al. (2016)) to make the system comprehensible for the human operator, which makes a parallel evaluation of all necessary simulations at once possible for modern desktop CPUs.

4.2 DOA Model Predictive Adaptive Automation

In the DOA case, the optimization domain $[0, 1]^2$ is uncountable. Since an infinite amount of H evaluations would be required, the LOA-MPAA cannot be extended to this case. As (1) is a nonlinear constrained optimization problem, the Karush-Khun-Tucker conditions (KKTC) are necessary conditions for optimality. We consider the derivative of the robot health using chain rule, as the gradient of

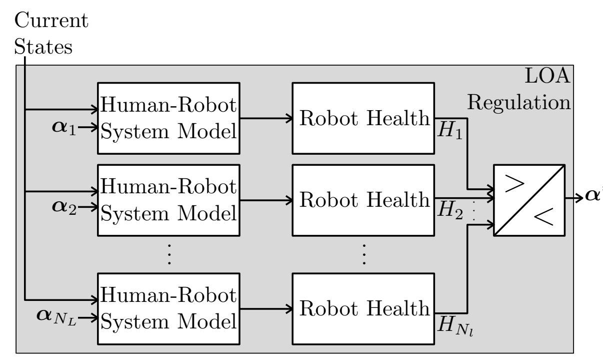

Fig. 2. LOA Regulation module.

the objective function forms the core of the KKTC. As H results from the probability of suffering P_suf of the robot, the derivative of P_suf wrt. $\boldsymbol{\alpha}$ plays a major role:

$$\frac{\mathrm{d}}{\mathrm{d}\boldsymbol{\alpha}} H\left(P_\mathrm{suf}\left(v_1\left(\boldsymbol{x}\left(\boldsymbol{\alpha}\right), \boldsymbol{\alpha}\right), \ldots, v_{N_\mathrm{v}}\left(\boldsymbol{x}\left(\boldsymbol{\alpha}\right), \boldsymbol{\alpha}\right)\right)\right) \tag{5}$$

$$= \frac{\mathrm{d}}{\mathrm{d}\boldsymbol{\alpha}} \int_{t_0}^{t_0+T_H} 1 - P_\mathrm{suf} \mathrm{d}t \tag{6}$$

$$= \int_{t_0}^{t_0+T_H} -\frac{\mathrm{d}P_\mathrm{suf}}{\mathrm{d}\boldsymbol{\alpha}} \mathrm{d}t \tag{7}$$

Due to the sum structure of P_suf, the overall derivative is a sum of the derivatives of the individual probabilities of suffering for each vital $P(s|v_i)$:

$$\frac{\mathrm{d}P_\mathrm{suf}}{\mathrm{d}\boldsymbol{\alpha}} = \frac{\mathrm{d}}{\mathrm{d}\boldsymbol{\alpha}} \eta \sum_{i=0}^{N_\mathrm{v}} P(s|v_i) = \eta \sum_{i=0}^{N_\mathrm{v}} \frac{\mathrm{d}P(s|v_i)}{\mathrm{d}\boldsymbol{\alpha}} \tag{8}$$

$P(s|v_i)$ are usually nonlinear, hence we have:

$$\frac{\mathrm{d}P(s|v_i)}{\mathrm{d}\boldsymbol{\alpha}} = \frac{\mathrm{d}P(s|v_i)}{\mathrm{d}v_i} \frac{\mathrm{d}v_i}{\mathrm{d}\boldsymbol{\alpha}} \tag{9}$$

In all of the original vitals presented in Ramesh et al. (2022), $\boldsymbol{\alpha}$ influences the vitals through the states:

$$\frac{\mathrm{d}v_i}{\mathrm{d}\boldsymbol{\alpha}} = \frac{\mathrm{d}v_i}{\mathrm{d}\boldsymbol{x}} \frac{\mathrm{d}\boldsymbol{x}}{\mathrm{d}\boldsymbol{\alpha}} \tag{10}$$

The influence on $\boldsymbol{x}$ stems from the influence on the inputs:

$$\frac{\mathrm{d}\boldsymbol{x}}{\mathrm{d}\boldsymbol{\alpha}} = \frac{\mathrm{d}}{\mathrm{d}\boldsymbol{\alpha}} \left(\int_{t_0}^{t_0+T_1} \dot{\boldsymbol{x}} \mathrm{d}t + \boldsymbol{x}_0 \right) = \int_{t_0}^{t_0+T_1} \frac{\mathrm{d}\dot{\boldsymbol{x}}}{\mathrm{d}\boldsymbol{u}} \frac{\mathrm{d}\boldsymbol{u}}{\mathrm{d}\boldsymbol{\alpha}} \mathrm{d}t \tag{11}$$

Finally, the inputs result from the arbitration which is parameterized by $\boldsymbol{\alpha}$:

$$\frac{\mathrm{d}\boldsymbol{u}}{\mathrm{d}\boldsymbol{\alpha}} = \frac{\mathrm{d}\boldsymbol{\Gamma}\left(\boldsymbol{u}_\mathrm{A}, \boldsymbol{u}_\mathrm{H}, \boldsymbol{\alpha}\right)}{\mathrm{d}\boldsymbol{\alpha}} \tag{12}$$

Thus, (5) results from the combination of (7) to (12). The concrete form of the gradient is application-specific and depends on the used arbitration, robot dynamics and the

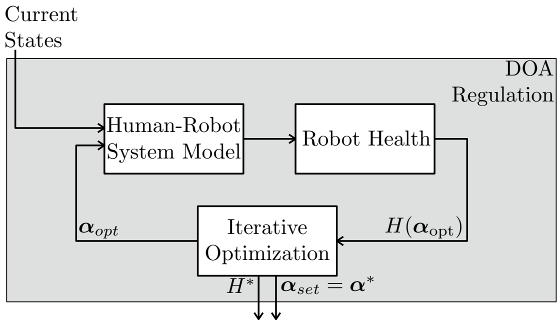

Fig. 3. DOA regulation module.

choice of robot vitals. Four different solutions are possible for Problem 2 depending on the features of the gradient:

Reduction of the problem Considering linear input blending, the following derivatives result with (4):

$$\frac{\mathrm{d}\boldsymbol{\Gamma}\left(\boldsymbol{u}_{\mathrm{A}}, \boldsymbol{u}_{\mathrm{H}}, \boldsymbol{\alpha}\right)}{\mathrm{d}\boldsymbol{\alpha}} = \begin{pmatrix} u_{\mathrm{A},1} - u_{\mathrm{H},1} & 0 \\ 0 & u_{\mathrm{A},2} - u_{\mathrm{H},2} \end{pmatrix} \tag{13}$$

The result in (13) is interesting for two reasons: First, it states that in a case where the human and the automation behave identically, robot health cannot be influenced by adjusting the DOA, hence the choice of DOA is arbitrary considering the information contained in the model presented above. Second, (13) is independent of $\boldsymbol{\alpha}$. Hence, given linear blending and a case where no expressions that are nonlinear in $\boldsymbol{\alpha}$ occur in H, the maximum of (1) will always be located on the boundaries of $\boldsymbol{\alpha}$. Therefore, traded control is the optimal solution to such a case and due to the countable set of possible DOAs, Problem 2 can be solved using the approach of Subsection 4.1.

Analytical solution If the overall gradient does depend on $\boldsymbol{\alpha}$ and the KKTC can be solved for $\boldsymbol{\alpha}$, candidate points for the optimal solution can be achieved this way. If more than one candidate point results, the optimum can be determined using a function evaluation similar to the procedure in Subsection 4.1. If feasible, this is a very computationally efficient solution.

Iterative, gradient-based solution If the gradient can be computed but solving the KKTC for $\boldsymbol{\alpha}$ is hard or infeasible, gradient-based iterative solvers can be used. This way, locally optimal solutions may result.

Iterative, gradient-free solution If the gradient cannot be computed e.g. in the case of piecewise-defined functions, gradient-free iterative solvers can be applied. While they may also generate locally optimal solutions and are often less computationally efficient compared to the gradient-based approaches, they are the most generally applicable solution to Problem (2) as they do not rely on a specific form of the optimization problem.

Hence, we chose to examine gradient-free solutions in this work. The resulting Model Predictive Adaptive Automation for the DOA case (DOA-MPAA) is shown in Fig. 3.

5. SIMULATION RESULTS

To evaluate the applicability of LOA-MPAA and DOA-MPAA, a proof-of-concept study was conducted in simulation. Both proposed systems were used for a collaborative tele-operation of a mobile robot in the scenario depicted in Fig. 4. The initial robot position is marked with a triangle indicating its heading, the goal point is marked with a large cross and the intermediate way-points are labeled as 1 to 6. While traversing towards the goal point, the robot faced four kinds of adverse conditions: 1) In the grey area, severe noise affected the laser scanner data, forcing the automation to reduce its range of commanded velocities to 20% of their magnitude during normal operations. 2) In the pink area, the operator got distracted and reduced their range of commanded velocities to 20% of their normal range. The laser scanners were still affected by noise in this area. However, the noise was less severe than in the grey area and the automation was able to use up to 60% of its normal input range. 3) While all other areas were flat, the orange area featured uneven terrain. The automation did not have information about the terrain. However, the human and the adaptive autonomy systems had this information a priori. For this reason, the human would add a conservative intermediate way-point between way-points 4 and 5 to avoid the orange area as indicated by the dashed line. 4) While traversing the blue area, unexpected behavior was induced into the robot's controller. Its input range was reduced to 20% without any environmental influences causing this. All other areas colored in white were not affected by performance degrading factors.

From the robot vitals presented in Ramesh et al. (2022), we included the three vitals most important for our study: The vital assessing the rate of change of distance from the navigational goal (ROCODO), the vital capturing the jerk along the z-axis of the robot, and the vital addressing the laser scanner noise. The rate of change $\dot{d}_{\mathrm{g}}$ of the ROCODO vital was computed as

$$\dot{d}_{\mathrm{g}} = \frac{1}{\left\|\boldsymbol{d}_{\mathrm{g}}\right\|_2} \boldsymbol{d}_{\mathrm{g}}^{\top} \begin{pmatrix} \beta \cos(\theta) \\ \beta \sin(\theta) \end{pmatrix} \text{ with } \boldsymbol{d}_{\mathrm{g}} = \begin{pmatrix} x_{\mathrm{g,i}} - x \\ y_{\mathrm{g,i}} - y \end{pmatrix}. \tag{14}$$

Here, $(x_{\mathrm{g,i}}, y_{\mathrm{g,i}})$ denotes the coordinates of the currently active way-point. The structure the vitals is chosen as in Ramesh et al. (2022) and the parameters of the mappings were fine-tuned to the scenario considered in this paper.

The robot dynamics were modeled as in (2), human behavior models both for the simulation model as well as the prediction models were based on extensive tele-operation experiments during the ARCHES project (Wedler et al. (2021)): When told to pursue a goal via way-points as described above, the operators usually first turned the robot until the correct heading had been reached and then

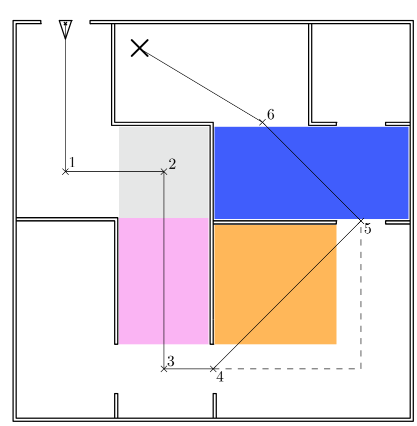

Fig. 4. Map of the considered scenario.

commanded velocities subsequently. This behavior was implemented by switching between a proportional controller for θ and a proportional controller for $\boldsymbol{d}_{\mathrm{g}}$ using the inputs ω and β. Apart from the different types of performance degradation, the model of the automation was identical to the one of the human as this structure was also used successfully in Wedler et al. (2021). Based on these models we set $\alpha = \alpha_1 = \alpha_2$ in (4) as neither the operator nor the automation influenced both inputs at the same time. All results were achieved with $T_p = 5\,\mathrm{s}$ and $T_s = 0.25\,\mathrm{s}$.

5.1 LOA-MPAA

Applying LOA-MPAA in an exemplary traded control case with $\Lambda = \{0, 1\}$, the trajectory depicted in Fig. 5a and the evolution of α depicted in Fig. 5c result. As Fig. 5a shows, the operator, automation and LOA-MPAA successfully manage to traverse through the white, grey, pink and blue areas reaching the goal position while avoiding the orange area. If human and automation performance predictions are equal, the automation is given control which happens in the white areas at the beginning and the end of the scenario as well as directly after passing the pink area. LOA-MPAA correctly assigns control to the human or the automation based on who is less impaired by the environmental influences in the grey, pink and blue area. Between way-point 4 and 5 a shift of control authority is performed to successfully leverage both the skill of the human to avoid the orange area as well as the skill of the automation to take the shortest path to way-point 5.

5.2 DOA-MPAA

DOA-MPAA is implemented using a patternsearch algorithm resulting in the plots presented in Fig. 5b and Fig. 5d. Like LOA-MPAA, it is able to coordinate the HMS to reach the goal successfully while also avoiding the orange area. Similar to LOA-MPAA, it assigns the control task to the automation if both the human and the automation are expected to perform equally (beginning, end and after pink area), slightly to the human in the grey and blue area and mostly to the automation in the pink area. Between the areas, smooth shifts of DOA result. During the traverse from way-point 4 to 5, a sharing of control spanning the whole range of DOAs occurs to trade off between avoiding the orange area and pursuing way-point 5.

Fig. 6 shows the evolution of the resulting predicted robot healths for MC, FA and the optimal solution α^* of the DOA-MPAA. It shows that neither a static operation in MC nor a static operation FA results in optimal health, but that regulating α during runtime both with LOA-MPAA and DOA-MPAA improves robot health. Due to the more granular adjustment, DOA-MPAA surpasses LOA-MPAA as α^* sometimes outperforms both options of LOA-MPAA.

6. CONCLUSION

In this paper, we contribute two model predictive adaptive automation systems using the robot health framework to quantify runtime performance degradation and adjust control authority to minimise the probability of task failure. While the first adaptive automation system shifts control between discrete, fixed Levels of Automation, the second system varies the Degree of Automation across the entire continuum thereby enabling granular adjustments. Simulation results indicate that the proposed systems are able to mitigate the effects of environmental adversities.

REFERENCES

Abbink, D.A., Carlson, T., Mulder, M., De Winter, J.C., Aminravan, F., Gibo, T.L., and Boer, E.R. (2018). A topology of shared control systems—finding common ground in diversity. *IEEE Transactions on Human-Machine Systems*, 48(5), 509–525.

Beer, J.M., Fisk, A.D., and Rogers, W.A. (2014). Toward a framework for levels of robot autonomy in human-robot interaction. *Journal of human-robot interaction*, 3(2).

Braun, C.A., Flad, M., and Hohmann, S. (2019). A continuous and quantitative metric for the levels of automation. *IFAC-PapersOnLine*, 52(19), 37–42.

Broggi, A., Cerri, P., Debattisti, S., Laghi, M.C., Medici, P., Molinari, D., Panciroli, M., and Prioletti, A. (2015). Proud—public road urban driverless-car test. *IEEE Transactions on Intelligent Transportation Systems*, 16(6), 3508–3519.

Cabrall, C.D., Janssen, N.M., and de Winter, J.C. (2018). Adaptive automation: Automatically (dis) engaging automation during visually distracted driving. *PeerJ Computer Science*, 4.

Chiou, M., Hawes, N., and Stolkin, R. (2021a). Mixed-initiative variable autonomy for remotely operated mobile robots. *ACM Transactions on Human-Robot Interaction (THRI)*, 10(4), 1–34.

Chiou, M., McCabe, F., Grigoriou, M., and Stolkin, R. (2021b). Trust, Shared Understanding and Locus of Control in Mixed-Initiative Robotic Systems. In *IEEE International Conference on Robot Human Interactive Communication (RO-MAN)*, 684–691. IEEE.

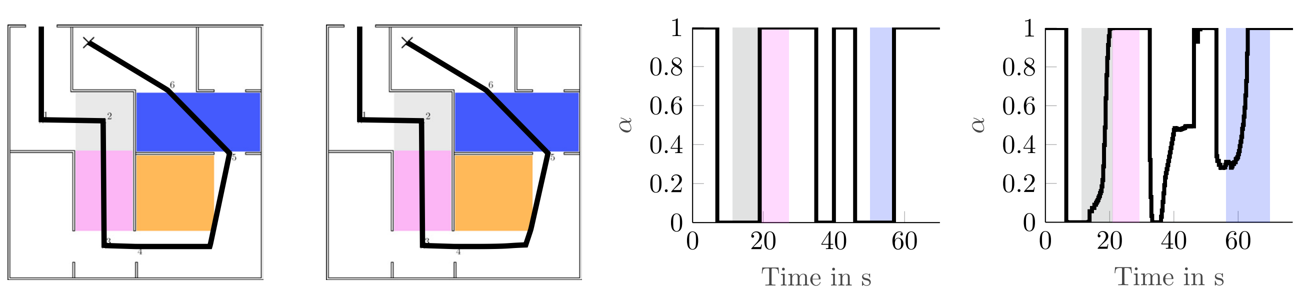

(a) Trajectory for LOA case. (b) Trajectory for DOA case. (c) Resulting LOAs. (d) Resulting DOAs.

Fig. 5. Simulation results. Background colors in Fig. 5c and 5d indicate the traverse of the equally colored areas in Fig. 5a and 5b.

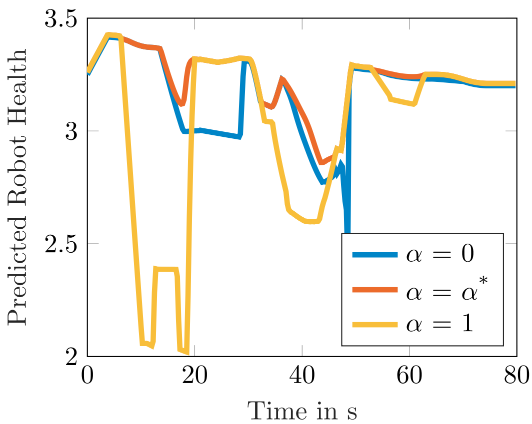

Fig. 6. Predicted robot health for different DOAs.

Chiou, M., Stolkin, R., Bieksaite, G., Hawes, N., Shapiro, K.L., and Harrison, T.S. (2016). Experimental analysis of a variable autonomy framework for controlling a remotely operating mobile robot. In *2016 IEEE/RSJ International Conference on Intelligent Robots and Systems (IROS)*, 3581–3588. IEEE.

Delmerico, J., Mintchev, S., Giusti, A., Gromov, B., Melo, K., Horvat, T., Cadena, C., Hutter, M., Ijspeert, A., Floreano, D., et al. (2019). The current state and future outlook of rescue robotics. *Journal of Field Robotics*, 36(7), 1171–1191.

Doroodgar, B., Liu, Y., and Nejat, G. (2014). A learning-based semi-autonomous controller for robotic exploration of unknown disaster scenes while searching for victims. *IEEE Transactions on Cybernetics*, 44(12).

Dragan, A.D. and S.Srinivasa, S. (2013). A policy-blending formalism for shared control. *The International Journal of Robotics Research*, 32(7), 790–805.

Gao, M., Oberländer, J., Schamm, T., and Zöllner, J.M. (2014). Contextual task-aware shared autonomy for assistive mobile robot teleoperation. In *2014 IEEE/RSJ International Conference on Intelligent Robots and Systems*, 3311–3318. IEEE.

Jiang, S. and Arkin, R.C. (2015). Mixed-initiative human-robot interaction: definition, taxonomy, and survey. In *2015 IEEE International conference on systems, man, and cybernetics*, 954–961. IEEE.

Miller, C.A. (2018). The risks of discretization: what is lost in (even good) levels-of-automation schemes. *Journal of Cognitive Engineering and Decision Making*, 12(1).

Milliken, L. and Hollinger, G.A. (2017). Modeling user expertise for choosing levels of shared autonomy. In *2017 IEEE International Conference on Robotics and Automation (ICRA)*, 2285–2291. IEEE.

Mostafa, S.A., Ahmad, M.S., and Mustapha, A. (2019). Adjustable autonomy: a systematic literature review. *Artificial Intelligence Review*, 51(2), 149–186.

Musić, S. and Hirche, S. (2017). Control sharing in human-robot team interaction. *Annual Reviews in Control*, 44.

Nikolaidis, S., Zhu, Y.X., Hsu, D., and Srinivasa, S. (2017). Human-robot mutual adaptation in shared autonomy. In *2017 12th ACM/IEEE International Conference on Human-Robot Interaction (HRI)*, 294–302. IEEE.

Pappas, P., Chiou, M., Epsimos, G.T., Nikolaou, G., and Stolkin, R. (2020). Vfh+ based shared control for remotely operated mobile robots. In *2020 IEEE International Symposium on Safety, Security, and Rescue Robotics (SSRR)*, 366–373. IEEE.

Petousakis, G., Chiou, M., Nikolaou, G., and Stolkin, R. (2020). Human operator cognitive availability aware mixed-initiative control. In *2020 IEEE International Conference on Human-Machine Systems (ICHMS)*.

Rakita, D., Mutlu, B., Gleicher, M., and Hiatt, L.M. (2019). Shared control–based bimanual robot manipulation. *Science Robotics*, 4(30).

Ramesh, A., Stolkin, R., and Chiou, M. (2022). Robot vitals and robot health: Towards systematically quantifying runtime performance degradation in robots under adverse conditions. *IEEE Robotics and Automation Letters*, 7(4), 10729–10736.

Rigter, M., Lacerda, B., and Hawes, N. (2020). A framework for learning from demonstration with minimal human effort. *IEEE Robotics and Automation Letters*, 5(2), 2023–2030.

Rothfuss, S., Chiou, M., Inga, J., Hohmann, S., and Stolkin, R. (2022). A Negotiation-Theoretic Framework for Control Authority Transfer in Mixed-Initiative Robotic Systems. In *IEEE International Conference on Systems, Man, and Cybernetics (SMC)*.

Ruff, H., Calhoun, G., Frost, E., Behymer, K., and Bartik, J. (2018). Comparison of adaptive, adaptable, and hybrid automation for surveillance task completion in a multi-task environment. In *Proceedings of the Human Factors and Ergonomics Society Annual Meeting*, volume 62, 155–159.

Sheridan, T.B. and Verplank, W.L. (1978). Human and computer control of undersea teleoperators. Technical report, Massachusetts Inst of Tech Cambridge Man-Machine Systems Lab.

Udupa, S., Kamat, V.R., and Menassa, C.C. (2021). Shared autonomy in assistive mobile robots: a review. *Disability and Rehabilitation: Assistive Technology*.

Vagia, M., Transeth, A.A., and Fjerdingen, S.A. (2016). A literature review on the levels of automation during the years. What are the different taxonomies that have been proposed? *Applied Ergonomics*, 53, 190–202.

Valero-Gomez, A., De La Puente, P., and Hernando, M. (2011). Impact of two adjustable-autonomy models on the scalability of single-human/multiple-robot teams for exploration missions. *Human factors*, 53(6), 703–716.

Wedler, A., Müller, M.G., Schuster, M., Durner, M., Brunner, S., Lehner, P., Lehner, H., Dömel, A., Vayugundla, M., Steidle, F., et al. (2021). Preliminary results for the multi-robot, multi-partner, multi-mission, planetary exploration analogue campaign on mount etna. In *Proceedings of the International Astronautical Congress*.

Wei, Z.G., Macwan, A.P., and Wieringa, P.A. (1998). A quantitative measure for degree of automation and its relation to system performance and mental load. *Human Factors*, 40(2), 277–295.

Xiao, X., Dufek, J., and Murphy, R.R. (2020). Robot risk-awareness by formal risk reasoning and planning. *IEEE Robotics and Automation Letters*, 5(2), 2856–2863.

Zieba, S., Polet, P., and Vanderhaegen, F. (2011). Using adjustable autonomy and human–machine cooperation to make a human–machine system resilient–application to a ground robotic system. *Information Sciences*, 181(3), 379–397.